Stability-oriented Optimization and Consensus Control for Inverter-based Microgrid

Weihang Yan, Wei Gao, David Wenzhong Gao
Dept. Electrical and Computer Engineering
University of Denver
Denver, USA
Weihang.yan@du.edu, Wenzhong.gao@du.edu

James Momoh
Dept. Electrical and Computer Engineering
Howard University
Washington D.C., USA

***Abstract*—In this paper, the small-signal model and stability-oriented consensus control scheme for inverter-based microgrid systems is proposed. By perturbating four identified dominant control parameters of inverter-based microgrid intentionally, the corresponding incremental matrix of microgrid system can be formed. Then, Matrix Perturbation Theory is employed in this paper to reduce the computational burden caused by repetitive calculations of system eigenvalues during stability analysis. Furthermore, the objective function is formulated based on the small-signal stability index and consensus index of microgrid system. Finally, the optimal control algorithm based on the joint application of Matrix Perturbation Theory and Artificial Fish Swarm Algorithm is introduced in this paper so that the stability and consensus rate of microgrid can be ensured. Besides, the effectiveness of proposed method can be verified in Matlab/Simulation results.**

***Index Terms*—Microgrids; Small-signal modeling; Matrix perturbation theory; Stability; Consensus.**

I. INTRODUCTION

Nowadays, wind power has become one of the cheapest renewable power generation technologies and solar power is expected to achieve grid parity in many countries in the near future. The development of both wind power and solar power generation technologies have significantly altered the control and operation of utilities [1]. Because of their widely available nature, renewable energy resources are suitable for distributed generation and utilization. Therefore, it is necessary to adopt microgrid as a platform to integrate renewable energy into the main electric grid. The inverter-based microgrid is considered as a type of microgrid network in which each distributed generator (DG) converts renewable energy through a voltage source inverter (VSI). So, the control of VSI has a vital role in operation of microgrid system [2]. Microgrids are expected to be more stable and reliable than traditional power system. However, many issues exist, such as stability of microgrid [3], accurate power sharing among DGs [4], consensus of DGs' voltages and frequencies [5], and lack of moment of inertia in VSI [6], [7], [8]. Among these issues, one of the major problems that receives attentions and interests is the stability-oriented consensus control of microgrid.

So far, some novel methods have been proposed in the literature to establish model and conduct stability analysis of inverter-based microgrid. Meanwhile, some optimal control methods have been also applied to microgrid system to reduce frequency and voltage oscillations. In reference [3], the small-signal model and stability of inverter-based microgrids are investigated under high penetration level of renewable energy. In order to improve the performance of microgrid, many efforts have been made in control parameters optimization such as optimal design of controller parameters and power sharing coefficients using particle swarm optimization [9]. Microgrids mentioned above are composed of inverters, power lines and loads, so the overall model that linearized around equilibrium point is complex and the order of the microgrid model is relatively high. Consequently, a large number of eigenvalues need to be derived in order to analyze the stability of microgrid systems. Matrix Perturbation Theory (MPT) is a fast method to calculate system eigenvalues so that iterative system analysis such as stability analysis can be conducted during system operation. It is mainly used to investigate the inherent characteristics and response of a system when the system parameters drift in a small range. MPT have been applied to the calculation of system eigenvalues and the stability analysis of microgrid with multiple DGs and loads [10]. From the results of using MPT, a high computing speed is achieved and the computational burden can also be reduced. On the other hand, Artificial Fish Swarm Algorithm (AFSA) is one of the best optimization techniques among swarm intelligence algorithms. It is inspired by the collective movement of fish and their various social behaviors. The global optimum is achieved through comparing individual local optima results in each fish swarm. AFSA has many advantages including high convergence rate, flexibility, fault tolerance and high accuracy [11].

In this paper, aiming at a series of microgrid operational issues including deviation of parameters of DGs, high order characteristics of microgrid model, and large computational burden of calculating microgrid system eigenvalues, a simplified small-signal model of microgrid system is established and stability-oriented optimization method using MPT and AFSA is proposed in order to solve the problem of consensus control of microgrid.

This work is supported by US National Science Foundation Grant 1711951 and 1429093.

II. MODELING OF MICROGRID SYSTEM

The structure of an inverter-based microgrid is shown in Fig.1.

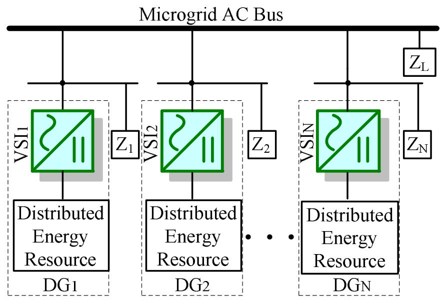

Figure 1. Structure of VSI-based microgrid

In Fig.1, the DG_i represents the ith DG in microgrid, which consists of DER and VSI. For instance, DER can be battery energy storage system. The main circuit and control system structure of DG is demonstrated in Fig.2.

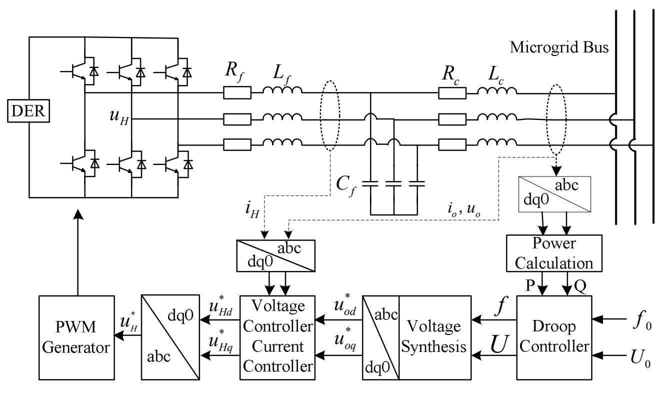

Figure 2. Main circuit and control system structure of DG

In Fig.2, according to Kirchhoff law and the Taylor series , the small-signal model of each part of DG can be derived. It can be defined $x_{dq}=[x_d \;\; x_q]^{\mathrm{T}}$ as the variables under d-q synchronously rotating reference frame. In later sections, x can be voltage u, current i or errors of voltage or current e_V, e_I. The mathematical model of inverter under d-q frame is presented in equation (1).

$$[\dot{u}_{odq},\dot{i}_{odq},\dot{i}_{Hdq}]^T = A_M[u_{odq},i_{odq},i_{Hdq}]^T + B_M[u_{Hdq}] + C_M[u_{Mdq}] \quad (1)$$

u_{Mdq} are voltage of microgrid bus. After linearizing the equation (1), the small-signal model of the main circuit of inverter system is obtained, as shown in (2).

$$\begin{aligned}[\Delta\dot{u}_{odq},\Delta\dot{i}_{odq},\Delta\dot{i}_{Hdq}]^T &= A_M[\Delta u_{odq},\Delta i_{odq},\Delta i_{Hdq}]^T \\ &+ B_M[\Delta u_{Hdq}] + C_M[\Delta u_{Mdq}] + D_M[\Delta\omega_g]\end{aligned} \quad (2)$$

Parameters U_{od} , U_{oq}, I_{od}, I_{oq}, I_{Hd} and I_{Hq} denote steady state values of LC filter output voltage, LC filter output current, and inverter leg current under d-q reference frame respectively. ω_g is the grid frequency in angular speed value. Systems matrix A_M, B_M, C_M, and D_M can be referred in paper [3], [5], [6]. The control system in Fig.2 is composed of droop power controller, voltage controller and current controller. Thus, the small-signal model of the power controller can be written as equation (3) and equation (4) [3].

$$\begin{bmatrix}\Delta\dot{P}\\ \Delta\dot{Q}\end{bmatrix} = A_p\begin{bmatrix}\Delta P\\ \Delta Q\end{bmatrix} + B_p\begin{bmatrix}\Delta u_{odq}\\ \Delta i_{odq}\\ \Delta i_{Hdq}\end{bmatrix} \quad (3)$$

$$\begin{bmatrix}\Delta\omega & \Delta u^*_{odq}\end{bmatrix}^T = C_p\begin{bmatrix}\Delta P & \Delta Q\end{bmatrix}^T \quad (4)$$

Here, P and Q are active power and reactive power of inverter output; ω is the output angular speed of the inverter; ω_c is cut-off frequency of low-pass filters, m_p and n_q are droop coefficients.

$$A_p = \begin{bmatrix}-\omega_c & 0\\ 0 & -\omega_c\end{bmatrix}, A_p = \begin{bmatrix}-m_p & 0\\ 0 & -n_q\end{bmatrix}$$

$$B_P = \begin{bmatrix}\omega_c I_{od} & \omega_c I_{oq} & \omega_c U_{od} & \omega_c U_{oq} & 0 & 0\\ \omega_c I_{oq} & -\omega_c I_{od} & -\omega_c U_{oq} & \omega_c U_{od} & 0 & 0\end{bmatrix}$$

PI regulators are used as the voltage controller and current controller. The mathematical model of dual-loop PI voltage and current controller are shown in equation (5). Here, e_{Vdq} and e_{Idq} are auxiliary parameters introduced.

$$\begin{cases} i^*_{Hdq} = Hi_{odq} - \omega_0 C_f u_{odq} + K_{pv}(u^*_{odq} - u_{odq}) + K_{iv}e_{Vdq}\\ u^*_{Hdq} = -\omega_0 L_f i_{Hdq} + K_{pc}(i^*_{Hdq} - i_{Hdq}) + K_{ic}e_{Idq}\\ e_{Vdq} = \int (u^*_{odq} - u_{odq})dt\\ e_{Idq} = \int (i^*_{Hdq} - i_{Hdq})dt \end{cases} \quad (5)$$

Using small-signal modeling technique to linearize equation (5), the small-signal model of voltage and current controller [12] can be obtained as shown in equation (6).

$$\begin{bmatrix}\Delta\dot{u}^*_{Hdq}\\ \Delta\dot{i}^*_{Hdq}\end{bmatrix} = A_C\begin{bmatrix}\Delta u_{odq}\\ \Delta i_{odq}\\ \Delta i_{Hdq}\end{bmatrix} + B_C\begin{bmatrix}\Delta i^*_{Hdq}\\ \Delta u^*_{odq}\end{bmatrix} + C_C\begin{bmatrix}\Delta e_{Idq}\\ \Delta e_{Vdq}\end{bmatrix} \quad (6)$$

$$A_C = \begin{bmatrix}A_{C1}\\ A_{C2}\end{bmatrix}_{4\times 6}, A_{C1} = \begin{bmatrix}0 & 0 & 0 & 0 & -K_{pc} & -\omega_0 L_f\\ 0 & 0 & 0 & 0 & \omega_0 L_f & -K_{pc}\end{bmatrix}$$

$$A_{C2} = \begin{bmatrix}-K_{pv} & -\omega_0 C_f & K & 0 & 0 & 0\\ \omega_0 C_f & -K_{pv} & 0 & K & 0 & 0\end{bmatrix}$$

$$B_C = \begin{bmatrix}B_{C1} & \mathbf{0}_{2\times 2}\\ \mathbf{0}_{2\times 2} & B_{C2}\end{bmatrix}_{4\times 4}, B_{C1} = \begin{bmatrix}K_{pc} & 0\\ 0 & K_{pc}\end{bmatrix}, B_{C2} = \begin{bmatrix}K_{pv} & 0\\ 0 & K_{pv}\end{bmatrix}$$

$$C_C = \begin{bmatrix}C_{C1} & \mathbf{0}_{2\times 2}\\ \mathbf{0}_{2\times 2} & C_{C2}\end{bmatrix}_{4\times 4}, C_{C1} = \begin{bmatrix}K_{ic} & 0\\ 0 & K_{ic}\end{bmatrix}, C_{C2} = \begin{bmatrix}K_{iv} & 0\\ 0 & K_{iv}\end{bmatrix}$$

In (6), K_{pv} and K_{iv} are proportional and integral coefficients of the voltage PI controller respectively. Meanwhile, K_{pc} and K_{ic} are proportional and integral coefficients of the current PI controller. $\mathbf{0}_{n\times n}$ denotes n×n order zero matrix.

Combining equation (2), (3), (4), and (6), the overall small-signal dynamic model of the ith DG system can be expressed as equation (7) and equation (8).

$$\left[\Delta \dot{x}_{Ii}\right] = A_i\left[\Delta x_{Ii}\right] + B_i\left[\Delta u_{Mdqi}\right] \tag{7}$$

$$\left[\Delta \omega_i \quad \Delta u_{odqi} \quad \Delta i_{odqi}\right]^T = C_i\left[\Delta x_{Ii}\right] \tag{8}$$

The state variables Δx_{Ii} equals to $[\Delta P_i, \Delta Q_i, \Delta u_{odi}, \Delta u_{oqi}, \Delta i_{odi}, \Delta i_{oqi}, \Delta i_{Hdi}, \Delta i_{Hqi}]^T$. Corresponding system matrix A_i, B_i, and C_i can be formulated below.

$$A_i = \begin{bmatrix} A_P & B_P \\ B_M B_{C1} B_{C2} C_P + C_M + D_M & A_M + B_M (B_{C1} A_{C2} + A_{C1}) \end{bmatrix}_{8\times 8} \tag{9}$$

$$B_i = \begin{bmatrix} \mathbf{0}_{2\times 2} \\ B_M \end{bmatrix}_{8\times 2}, C_i = \begin{bmatrix} M_1 C_P & \mathbf{0}_{1\times 6} \\ \mathbf{0}_{4\times 2} & M_2 \end{bmatrix}_{5\times 8}, M_1 = \begin{bmatrix} 1 \\ 0 \end{bmatrix}^T, M_2 = \begin{bmatrix} 1 & & & & \\ & 1 & & & \mathbf{0}_{4\times 2} \\ & & 1 & & \\ & & & 1 & \end{bmatrix}$$

Equation (7) presents a 8th order small-signal model of a DG system. Assuming inverter-based microgrid consists of N DGs. By integrating line impedances and according to equation (7), the small-signal model of overall microgrid can be obtained in equation (10).

$$\left[\Delta \dot{\mathbf{x}}\right] = A_{mg}\left[\Delta \mathbf{x}\right] + B\left[\Delta \mathbf{u}_{Mdq}\right] \tag{10}$$

In sum, the state variables of overall microgrid are $\Delta \boldsymbol{x}=[\Delta \boldsymbol{x}_{I1}, \Delta \boldsymbol{x}_{I2}, \ldots, \Delta \boldsymbol{x}_{IN}]^T$. The system matrix of microgrid is shown in (11).

$$A_{mg} = \begin{bmatrix} A_1 & \mathbf{0}_{8\times 8} & \ldots & \mathbf{0}_{8\times 8} \\ \mathbf{0}_{8\times 8} & A_2 & \ldots & \mathbf{0}_{8\times 8} \\ \ldots & \ldots & \ldots & \ldots \\ \mathbf{0}_{8\times 8} & \mathbf{0}_{8\times 8} & \ldots & A_N \end{bmatrix} \tag{11}$$

III. EIGENVALUE ANALYSIS OF MICROGRID

The stability and dynamic performance of microgrid system can be analyzed through obtaining the eigenvalues of microgrid system matrix. By applying perturbations on control parameters of DGs and along with the distribution of eigenvalues of microgrid system, it can be concluded that the changes of K_{pv}, K_{ic}, m_p, n_q have great impact on the stability of overall inverter-based microgrid [13]. Therefore, control parameters K_{pv}, K_{ic}, m_p, n_q can be identified as the dominant control parameters of microgrid system. Since a microgrid is made up of multiple DGs, and the order of microgrid system matrix A_{mg} equals to 8 times of the total number of DGs in the inverter-based microgrid, the computational process of calculating eigenvalues of microgrid system is very complex and slow. In order to solve this issue, this paper employs MPT to speed up the calculation of microgrid system eigenvalues.

During the optimization and operational process of microgrid system, the system matrix changes constantly so that the eigenvalues of the system matrix have to be recalculated and solved repeatedly in order to derive the optimal control parameters. This results in a great deal of repetitive calculations. Alternatively, according to paper [10], the system matrix A_{mg} can be obtained based on MPT with only calculating the incremental matrix ΔA_{mg} when base matrix $A_{\mathrm{mg}0}$ is considered as constant. Equation (12) gives the expression of the system matrix A_{mg} when first-order perturbation is applied. Thus, eigenvalues for the perturbed system can be calculated more rapidly. Meanwhile, the calculation burden for stability-oriented optimization and control is greatly reduced, and the computation speed for system optimization can be improved.

$$A_{mg} = A_{mg0} + \Delta A_{mg} \tag{12}$$

According to identified dominant control parameters of inverter-based microgrid above, the incremental matrix can be generated when perturbations are applied on dominant control parameters, as shown in equation (13).

$$\Delta A_{mg} = \begin{bmatrix} \sum_{j=1}^{6} \Delta A_{1j} & \mathbf{0}_{8\times 8} & \ldots & \mathbf{0}_{8\times 8} \\ \mathbf{0}_{8\times 8} & \sum_{j=1}^{6} \Delta A_{2j} & \ldots & \mathbf{0}_{8\times 8} \\ \ldots & \ldots & \ldots & \ldots \\ \mathbf{0}_{8\times 8} & \mathbf{0}_{8\times 8} & \ldots & \sum_{j=1}^{6} \Delta A_{Nj} \end{bmatrix} \tag{13}$$

In equation (13) and referring to equation (9), ΔA_{ij} can be defined as the incremental matrix for the ith DG system when the dominant control parameters are perturbed. The detailed representations for each diagonal element of incremental matrix (13) can be presented in (14).

$$\Delta A_{ij} = \begin{cases} \Delta A_{i1}(K_{pv}) & j = 1, K_{pv} \text{ is perturbed} \\ \Delta A_{i2}(K_{ic}) & j = 2, K_{ic} \text{ is perturbed} \\ \Delta A_{i3}(m_p) & j = 3, m_p \text{ is perturbed} \\ \Delta A_{i4}(n_q) & j = 4, n_q \text{ is perturbed} \\ i = 1, 2, \ldots, N & i \text{ is number of DG in microigrid.} \end{cases} \tag{14}$$

As we can see in (14), the variation of one dominant control parameter can result in the changes for multiple block matrixes. Similarly, perturbed eigenvalues and eigenvectors can be decomposed into initial eigenvalue $\lambda_0^{(r)}$ and initial eigenvector $\upsilon_0^{(r)}$ with their first-order perturbation $\lambda_1^{(r)}$ and $\upsilon_1^{(r)}$. Here (r) denotes the rth eigenvalue or eigenvector of system matrix A_{mg}.

$$\begin{cases} \lambda^{(r)} = \lambda_0^{(r)} + \lambda_1^{(r)} \\ \upsilon^{(r)} = \upsilon_0^{(r)} + \upsilon_1^{(r)} \end{cases} \tag{15}$$

By substituting (14) into (13), ΔA_{mg} can be calculated and the eigenvalues and eigenvectors of system matrix A_{mg} can also be obtained according to MPT [10]. Equations (16) and (17) express the eigenvalues and eigenvectors of system matrix A_{mg} calculated through MPT.

$$\begin{cases} \lambda_1^{(r)} = (\upsilon_0^{(s)})^T \Delta A_{mg} \upsilon_0^{(r)} \\ \upsilon_1^{(r)} = \sum_{\substack{s=1 \\ s\neq r}}^{n} (\upsilon_0^{(s)})^T \Delta A_{mg} \upsilon_0^{(r)} \upsilon_0^{(s)} / (\lambda_0^{(r)} - \lambda_0^{(s)}) \end{cases} \tag{16}$$

$$\begin{cases} \lambda_1^{(r)} = (\upsilon_0^{(r)})^T \Delta A_{mg} \upsilon_0^{(r)} \\ \upsilon_1^{(r)} = \displaystyle\sum_{s=1,r+1\cdots,r+m-1(s\neq r)}^{n} \frac{\sum_{j=1}^{m} N_j^{(r)}((\upsilon_0^{(s)})^T \Delta A_{mg} \upsilon_{j0}^{(r)})}{\lambda_0^{(r)} - \lambda_0^{(s)}} \upsilon_0^{(s)} \end{cases} \tag{17}$$

IV. OPTIMAL CONTROL OF INVERTER-BASED MICROGRID

In this paper, the combination of MPT and AFSA is employed in order to accomplish the two-level optimization and control for inverter-based microgrid. In the preliminary optimization, the stability-oriented optimization model is established for proposed microgrid system. Optimized dominant control parameters can be derived and programmed into DG's controller through the joint application of MPT and AFSA. Then, for the secondary optimization, the consensus-oriented optimization model is established based on the frequency and voltage consensus law of inverter-based microgrid. AFSA is adopted to carry out the consensus-oriented optimization of microgrid. Therefore, optimized reference voltage and frequency f_0, U_0 of each DG can be obtained while maintaining the stability of proposed microgrid. The objective functions of inverter-based microgrid J_1 and J_2 with respect to the system eigenvalues and consensus errors are presented in equation (18).

$$\begin{cases} J_1 = \min \displaystyle\sum_{\forall R_e^{(r)} \geq 0, r=1}^{L} E_1^{(r)}(m_p, n_q, K_{ic}, K_{pv}) \\ J_2 = \min \displaystyle\sum_{k=1}^{N} \boldsymbol{\beta}^T \mathbf{E}_2^{(k)} \end{cases} \tag{18}$$

In (18), J_1 corresponds to the stability-oriented optimization model and J_2 corresponds to the consensus-oriented optimization model. Besides, L is the total number of eigenvalues of microgrid system matrix A_{mg}. $\boldsymbol{\beta}=[\beta_1, \beta_2, \beta_3, \beta_4]^T$ are weight coefficients. N is the number of DGs in microgrid. As a result, $E_1^{(r)}$ can be defined in equation (19). Here, $E_1^{(r)}$ can be considered as stability index of the rth eigenvalue, with $E_1^{(r)}$ equal to real part of the rth eigenvalue $R_e^{(r)}$. In inverter-based microgrid system, it can be summarized that $R_e^{(r)}$ is determined in a great extent by the dominant control parameters K_{pv}, K_{ic}, m_p, n_q and a minimum value of stability-oriented objective function J_1 leads to a more stable microgrid system.

$$\begin{cases} E_1^{(r)}(m_p, n_q, K_{ic}, K_{pv}) = R_e^{(r)} \\ R_e^{(r)} = R_e(\lambda_0^{(r)} + \lambda_1^{(r)}) \end{cases} \tag{19}$$

For the sub-objective function J_2, function vector $\mathbf{E}_2^{(k)}$ for the kth DG can be expressed in equation (20).

$$\begin{bmatrix} E_{21}^{(k)} \\ E_{22}^{(k)} \\ E_{23}^{(k)} \\ E_{24}^{(k)} \end{bmatrix} = \begin{bmatrix} (f_n^k - m_p^k P^k - f_0)^2 \\ \displaystyle\sum_{j=1, j\neq k}^{N} a_{ij}[(f_n^k - m_p^k P^k) - f^j]^2 \\ (U_n^k - n_q^k Q^k - U_0)^2 \\ \displaystyle\sum_{j=1, j\neq k}^{N} a_{ij}[(U_n^k - n_q^k Q^k) - U^j]^2 \end{bmatrix} \tag{20}$$

Here, $E_{21}^{(k)}$, $E_{23}^{(k)}$ define the frequency and voltage errors of the kth DG comparing with system nominal values and $E_{22}^{(k)}$, $E_{24}^{(k)}$ define the frequency and voltage consensus errors with comparison to all neighboring DGs of the kth DG [5], [6] in microgrid system. f_0^k, U_0^k are optimal reference frequency and voltage amplitude of the kth DG. f^j, U^j are feedback frequency and voltage amplitude respectively from the jth ($j\neq k$) DG.

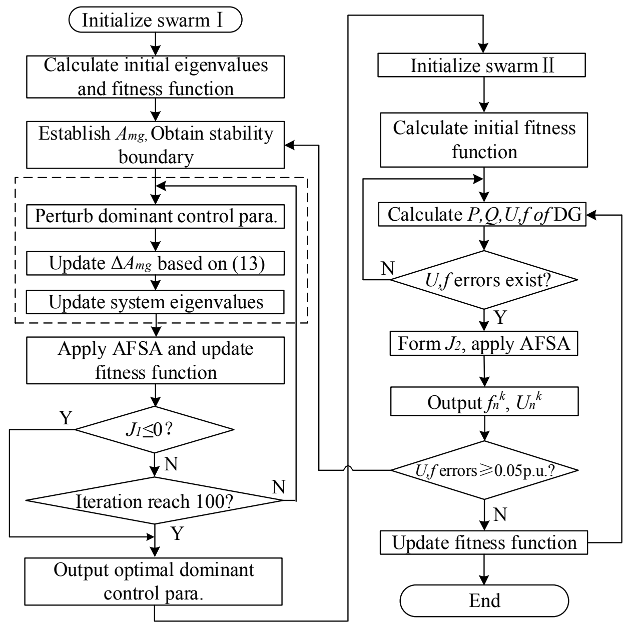

Figure 3. Overall optimization flow chart of inverter-based microgrid

Fig. 3 gives the overall two-level optimization flow chart of inverter-based microgrid. Left-hand side part of the flow chart illustrates stability-oriented optimization and right-hand side of the flow chart demonstrates consensus-oriented optimization. Based on equation (18), fitness function can be selected by employing the combination of J_1 and J_2. The operation of an unstable inverter-based microgrid can be converted into its stable mode after the first level of optimization. Then, the overall two-level optimization can circulate iteratively during the operation of microgrid such that the system matrix can be updated after major disturbance as well as the optimal control setting can be reconfigured repetitively.

V. NUMERICAL SIMULATION EXAMPLE

In this section, the simulation example regarding stability-oriented optimization and consensus control for an inverter-based microgrid is presented and conducted. The system parameters of the inverter-based microgrid can be presented in Tab.1.

TABLE I. PARAMETERS OF CIRCUIT AND INITIAL VALUE

Parameter	value	Parameter	value
RL_1, RL_2	25Ω	K_{pv}	0.8
L_{L1}, L_{L2}	2e-4H	K_{iv}	200
R_L	20Ω	K_{pc}	8
L_L	1.5e-4H	K_{ic}	1200
R_{f1}, R_{f2}	0.04Ω	m_p	3e-4
L_{f1}, L_{f2}	1.5e-3H	n_q	1e-2

C_{f1}, C_{f2}	1600e-6F	U_0	311V
R_{c1}, R_{c2}	0.05Ω	U_M	311V
L_{c1}, L_{c2}	0.7e-3H	I_0	25A
ω_0	314	ω_c	50

The inverter-based microgrid tested, as shown in Fig. 1, consists of three DGs, three DG's local loads and one public load located at the microgrid AC bus. In order to verify the accuracy of eigenvalues calculated using MPT, Fig. 4 compares the eigenvalues of a microgrid system matrix A_{mg} derived from MPT and QR algorithms [14] respectively. In Fig.4, the distributions of system eigenvalues which starts from two different initial conditions are shown. it can be concluded that the distribution of eigenvalues calculated by MPT almost overlaps the distribution of eigenvalues calculated by QR. Therefore, MPT can be verified as accurate for computing the eigenvalues of microgrid system meanwhile fast computational speed can be achieved.

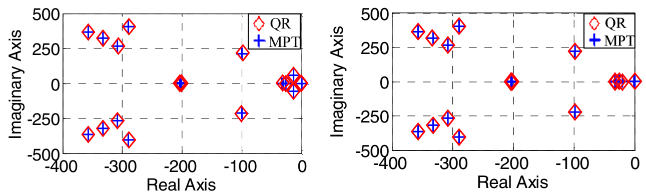

Figure 4. Eigenvalues' computation results using MPT and QR

The initial control settings lead to an unstable inverter-based microgrid system, where $[m_p, n_q, K_{pv}, K_{ic}]^T$=[3e-4, 1e-2, 0.8, 1200]^T. As the joint application of MPT and AFSA proceeds, the unstable eigenvalues of microgrid system are shifted to the left half plane by optimizing the four dominant control parameters. Finally, dominant control parameters are converged to $[m_p, n_q, K_{pv}, K_{ic}]^T$=[9.5e-6, 1.42e-4, 0.56, 1621.10]^T. On the other hand, the secondary consensus-oriented optimization is able to drive frequency and voltage consensus errors asymptotically converge to zero. Fig. 5 illustrates the trajectory of fitness function of proposed inverter-based microgrid, which shows convergence after 24 iterations.

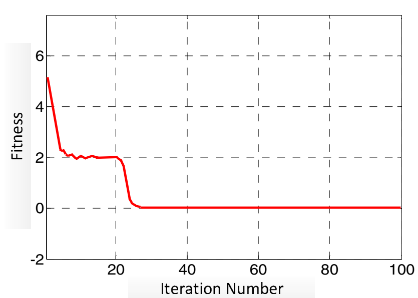

Figure 5. Optimization curve of the objective function J_1+J_2

Fig. 6 and Fig. 7 demonstrate the frequency and voltage responses of individual DG respectively when microgrid public load is increased. As we can see, DG systems can operate in their stable mode with the assistance of stability-oriented optimization. Moreover, the output frequencies and voltages of individual DG are able to restore to nominal values cooperatively within a relatively short settling time, which means that microgrid consensus errors can be eliminated through the consensus-oriented optimization.

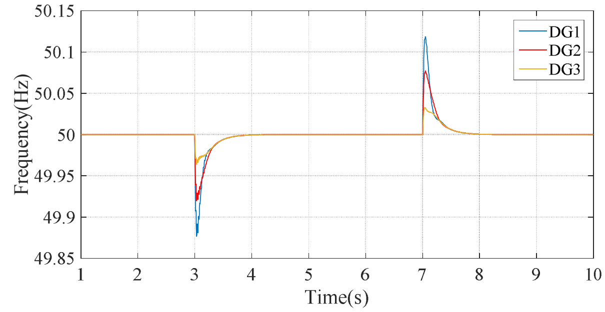

Figure 6. Frequency response of microgrid DGs

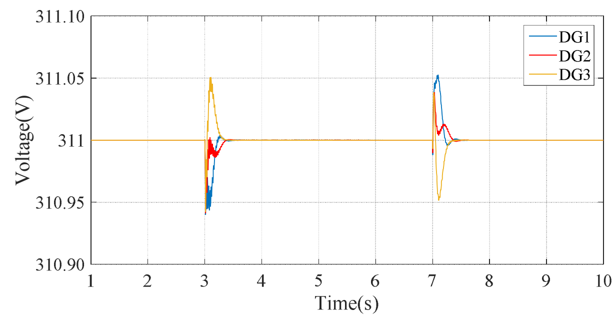

Figure 7. Voltage response of microgrid DGs

VI. Conclusion

In this paper, individual DG systems are modeled so that the complete small-signal model of the inverter-based microgrid can be obtained. Four dominant control parameters that affect the stability of an inverter-based microgrid are also identified. Based on obtained system model, the stability-oriented optimization model and the consensus-oriented optimization model are established respectively and the joint application of MPT and AFSA is employed to achieve cooperative voltage and frequency restoration. Both theoretical analysis and simulation results show that the increment of system matrix generated by perturbation of system matrix of microgrid can be rapidly calculated using MPT. Therefore, the computational burden of eigenvalues can be greatly reduced and the optimal control performance can be improved. Finally, the frequency and voltage consensus control of all DGs in microgrid system can be achieved.

References

[1] Z. Wu, D. W. Gao, H. Zhang, S. Yan, and X. Wang, "Coordinated control strategy of battery energy storage system and PMSG-WTG to enhance system frequency regulation capability," *IEEE Trans. on Sustainable Energy*, vol. 8, pp. 1330-1343, Jul. 2017.

[2] W. Yan, S. Yan, and D. W. Gao, "A voltage perturbation control of VSI with estimator in weak microgrid," in *Proc. 2015 Chinese Control and Decision Conf. (CCDC)*, pp.601-606.

[3] N. Pogaku, M. Prodanovic, and T. C. Green, "Modeling, analysis and testing of autonomous operation of an inverter-based microgrid," *IEEE Trans. on Power Electronics*, vol.22, pp.613-625, Mar. 2007.

[4] M. J. Hossain, H. R. Pota, M. A. Mahmud, M. Aldeen, "Robust control for power sharing in microgrids", *IEEE Trans. on Sustainable Energy*, vol.6, pp.1067-1077, Jul. 2015.

[5] A Bidram, A Davoudi, F. L. Lewis, and J. M. Guerrero, "Distributed cooperative secondary control of microgrids using feedback linearization", *IEEE Trans. on Power Systems*, vol.28, pp.3462-3470, 2013.

[6] W. Yan, W. Gao, T. Gao, D. W. Gao, S. Yan, and J. Wang, "Distributed cooperative control of virtual synchronous generator based microgrid, in *Proc. 2017 IEEE International Conference on Electro Information Technology (EIT)*, pp.506-511.

[7] H. Jiang, Y. Zhang, J. J. Zhang, D. W. Gao and E. Muljadi, "Synchrophasor-based auxiliary controller to enhance the voltage stability of a distribution system with high renewable energy penetration," *IEEE Transactions on Smart Grid*, vol. 6, pp. 2107-2115, Jul. 2015.

[8] X. Wang, W. Gao, J. Wang, Z. Wu, W. Yan, V. Gevorgian, Y. Zhang, E. Muljadi, M. Kang, M. Hwang, and Y. C. Kang, "Assessment of system frequency support effect of PMSG-WTG using torque-limit-based inertial control," in *Proc. 2016 IEEE Energy Conversion Congress and Exposition (ECCE)*, pp.1-6.

[9] M. A. Hassan, M. A. Abido, "Optimal design of microgrids in autonomous and grid-connected modes using particle swarm optimization, " *IEEE Trans. on Power Electronics*, vol.26, pp.755-769, Mar. 2011.

[10] Y. Li, D. W. Gao, and E. Muljadi, "Novel approach for calculation and analysis of eigenvalues and eigenvectors in microgrids", in *Proc. 2014 Clemson University Power Systems Conf.*, pp.1-5.

[11] M. Neshat, G. Sepidnam, M. Sargolzaei, M. Sargolzaei, and A. N. Toosi, "Artificial fish swarm algorithm: a survey of the state-of-the-art", hybridization, combinatorial and indicative applications," *Artificial Intelligence Review*, vol.42, pp. 965-997, May. 2014.

[12] M. N. Marwali, and A. Keyhani, "Control of distributed generation systems – part I: voltage and currents control," *IEEE Trans. on Power Electronics*, vol.19, pp. 1541-1550, Nov. 2004.

[13] S. Yan, W. Yan, W. Gao, " A Multi-parameter Rapid Optimization Method of Inverter-based Microgrid," in *Proc. 2018 IEEE PES Transmission and Distribution Conference & Exposition (T&D 2018)*, in press.

[14] J. Ma, Z. Y. Dong and P. Zhang, "Comparison of BR and QR eigenvalue algorithms for power system small signal stability analysis, "*IEEE Trans. on Power Systems*, vol. 21, pp. 1848-1855, Nov. 2006.